Chemistry–A European Journal
Research Article
doi.org/10.1002/chem.202300116
Chemistry Europe
European Chemical Societies Publishing
www.chemeurj.org

Silver-Based Terpyridine Complexes as Antitumor Agents

María Gil-Moles,[a] M. Elena Olmos,[a] Miguel Monge,[a] Manuel Beltrán-Visiedo,[b] Isabel Marzo,[b] José M. López-de-Luzuriaga,*[a] and M. Concepción Gimeno*[c]

Abstract: Silver complexes bearing substituted terpyridine or tetra-2-pyridinylpyrazine ligands have been prepared and structurally characterised. The study of the anticancer properties of silver complexes with this type of ligands is scarce, despite the possibilities of combining the properties of the metal and the ability of the ligands for DNA binding. Here, the antiproliferative activity, stability, CT-DNA binding, and mechanism of cell death of these types of derivatives are studied. High cytotoxicity against different tumour cells was observed, and, more important, a great selectivity index has been detected between tumour cells and healthy lymphocytes T for some of these compounds. The CT-DNA interaction study has shown that these derivatives are able to interact with CT-DNA by moderate intercalation. Furthermore, cell death studies indicate that these derivatives promote the apoptosis by a mitochondrial pathway.

Introduction

During the last years, the interest in the medical inorganic chemistry has greatly increased after the discovery of the anticancer activity of cisplatin, carboplatin, and oxaliplatin.[1] Although many other platinum compounds have been synthetised, the toxicity, side effects, reduction of the immunity and drug resistance of this type of compounds limit their application in medicine.[2] Therefore, the design of new therapeutic drugs with non-platinum complexes responsible for the antiproliferative effects have been increasingly studied by many researchers. Several other metal complexes have been found to display promising cytotoxic activity such as gold, ruthenium or copper, among others.[3–11]

Silver is an element present in the human body in very low concentration, usually bonded to proteins. It has a great biological compatibility and is easily eliminated. The antimicrobial properties of silver compounds and nanoparticles have been largely known and have been incorporated into medicinal drugs because of their high antimicrobial activity.[12]

However, in the last years it has been observed that the silver complexes show good cytotoxic activity against many cancer cells.[13] In addition, the synthesis of silver(I) compounds has gained importance in the last years due to their lower toxic effects on healthy cells and promising anticancer effects.[14]

Some studies have demonstrated that several silver derivatives with O-, N-, P-, S-donor ligands and especially with N-heterocyclic carbenes exhibit high cytotoxic activity in diverse human tumour cells.[13a,15] The complexes with functionalised pyridines, as well as other ancillary ligands such as carboxylate, amino acids, sulfur or phosphorus donor groups, highlight the development of novel anticancer drugs.[14–16] Mechanisms of action of silver(I) derivatives are not clear yet, but the studies indicate an apoptotic cell death, generation of ROS, DNA binding and cleavage, and inhibition of the topoisomerase enzyme as the most probable mechanisms.[13–16]

Despite the fact that helical metal-constituted architectures with nitrogen donor ligands were found to be effective in terms of antitumor activity,[17] biological studies that concern silver(I) terpyridine are relatively scarce.[18] In addition, in spite that several silver(I) tetra-2-pyridinylpyrazine complexes have been reported,[19] no biological studies have been described for these compounds, and the existing biological studies have been reported for different metals.[20]

Considering that terpyridine complexes have been found to be efficient intercalating DNA agents and have shown inhibitory activity on cancer cells in vitro,[18] together with the excellent properties shown by silver complexes as commented earlier and as we have previously reported,[21] our aim is to study the combination of both fragments in the search of complexes with antitumor activity.

[a] Dr. M. Gil-Moles, Prof. Dr. M. E. Olmos, Prof. Dr. M. Monge, Prof. Dr. J. M. López-de-Luzuriaga
Departamento de Química
Universidad de La Rioja
Centro de investigación de Síntesis Química (CISQ)
Complejo Científico-Tecnológico, 26004-Logroño (Spain)
E-mail: josemaria.lopez@unirioja.es

[b] M. Beltrán-Visiedo, Prof. Dr. I. Marzo
Departamento de Bioquímica y Biología Celular
Universidad de Zaragoza-CSIC
50009 Zaragoza (Spain)

[c] Prof. Dr. M. Concepción Gimeno
Departamento de Química Inorgánica
Instituto de Síntesis Química y Catálisis Homogénea (ISQCH)
CSIC-Universidad de Zaragoza, 50009 Zaragoza (Spain)
E-mail: gimeno@unizar.es

Supporting information for this article is available on the WWW under https://doi.org/10.1002/chem.202300116

Results and Discussion

With the purpose to study the antitumor properties of several silver(I) complexes with terpyridine-based ligands, we proposed the formation of complexes with the ligands collected in Figure 1, 4-substituted terpyridines with donor or acceptor ligands **L1**--**L3**, and the related tetra-2-pyridinylpyrazine **L4**.

Homoleptic dinuclear silver complexes and mononuclear species with a phosphine as ancillary ligand have been prepared and characterised. The reaction of ligands **L1**–**L3** with a solution of $AgBF_4$ in diethyl ether afforded the dinuclear species **1**–**3** in which is proposed that the terpyridine ligand is bridging both metal centres in an analogous fashion to similar compounds previously described (see Scheme 1).[22]

Complexes **4**–**6** bearing an ancillary triphenylphosphine ligand were synthesised by reaction of the solvated complex $[Ag(S)PPh_3]BF_4$ (see experimental section) (S = solvent) with the different terpyridine ligands in equimolar amounts. In contrast, when the auxiliary ligand is trimethylphosphine (PMe_3), the complex $[Ag(S)PMe_3]BF_4$ is not stable, and it is necessary to treat a freshly prepared solution of this compound *in situ* and under argon conditions with ligands **L1**–**3** to provide complexes **7**–**9** (see Scheme 2).

In a similar manner, the tetra-2-pyridinylpyrazine derivative reacts with the silver complexes in a 1:2 molar ratio to afford the dinuclear species **10** and **11** (Scheme 3).

All the complexes have been characterised by elemental analysis, IR, MALDI mass spectra, and NMR spectroscopy (see experimental section), and the spectroscopic and analytical data are in agreement with the proposed stoichiometries.

MALDI-TOF mass spectra have been recorded and, in all cases, the isotopic distributions found experimentally agree with the theoretical ones. When no ancillary ligand is used it is possible to detect the following peaks by MALDI-TOF(+) *m/z*: $[Ag(4'\text{-X-terpy})]^+ = 340$ (**1**), 370 (**2**), 376 (**3**) and $[Ag(4'\text{-X-terpy})_2]^+ = 573$ (**1**), (**2**), 643 (**3**). In cases where PPh_3 is used, MALDI-TOF(+) *m/z*: $[Ag(PPh_3)(4'\text{-X-terpy})]^+ = 602$ (**4**), 632 (**5**), 638 (**6**) and $[Ag(PPh_3)(\text{tetra-2-pyridinylpyrazine})]^+ = 757$ (**10**). In compounds where PMe_3 is used, the following peaks have been detected. MALDI-TOF(+) *m/z*: $Ag(PMe_3)(4'\text{-X-terpy})]^+ = 416$ (**7**), 446 (**8**), 452 (**9**) and $[Ag(PMe_3)(\text{ tetra-2-pyridinylpyrazine})]^+ =$ 571 (**11**).

The ^1H NMR spectra of the new compounds display the expected resonances for the N-donor ligands as well as those corresponding to triphenyl- (**4**, **5**, **6**) or trimethylphosphine (**7**, **8**, **9**), whose relative integration indicates that only one phosphine group is coordinated to the silver centre. The $^{31}P\{^1H\}$ NMR spectra of the silver(I) complexes with phosphine ligands **4**–**6** display a fluxional behaviour in solution, showing two broad signals at room temperature, which are indicative of an average coupling of the ^{31}P nuclei with the ^{107}Ag and ^{109}Ag ones. In contrast, for complexes **7**–**9** only one broad resonance is observed. At low temperature, a different behaviour can be observed depending on the type of phosphine ligand (see Supporting Information Figures S1–S4). For complexes **4**–**6**, which contain PPh_3, the $^{31}P\{^1H\}$ NMR spectra at 220 K consist in two doublets due to the coupling of the ^{31}P nuclei with both silver isotopomers; and the corresponding coupling constants are characteristic of silver monophosphine derivatives contain-

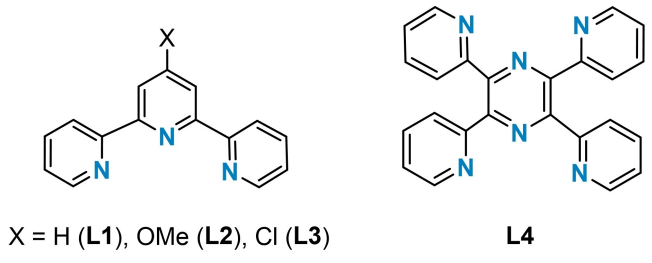

Figure 1. Terpyridine-based ligands used in this study.

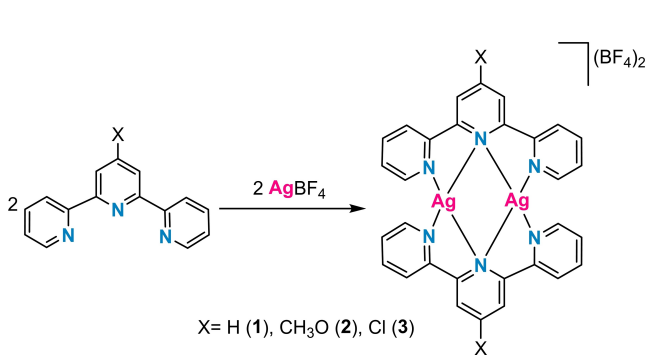

Scheme 1. Synthesis of complexes **1**–**3.**

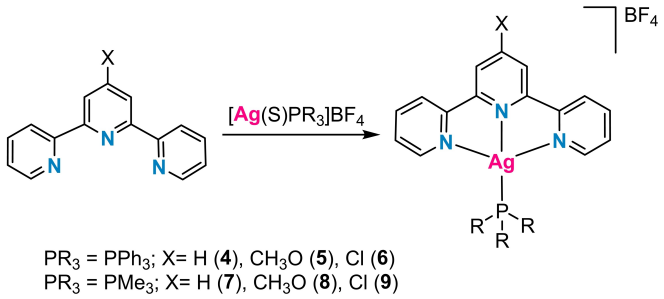

Scheme 2. Synthesis of complexes **4**–**9**.

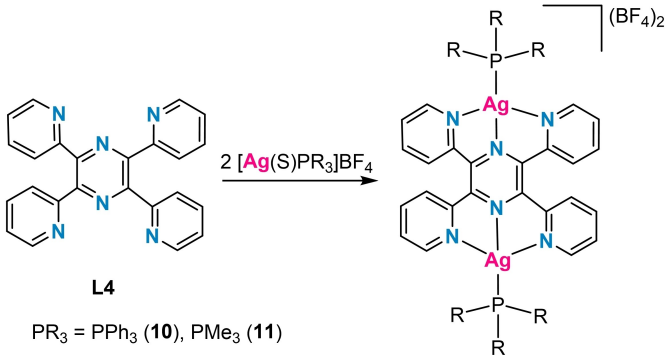

Scheme 3. Synthesis of complexes **10**–**11**.

ing the fragment $[Ag(PPh_3)]^+$. In contrast, the $^{31}P\{^1H\}$ NMR spectra of the trimethylphosphine complexes **7** and **8** at 190 K (CD_2Cl_2) display unresolved doublets (from which only the average coupling constant can be determined), and only for complex **9** two doublets are clearly observed. This different behaviour in solution for complexes **7** and **8** is probably due to the faster fluxional motion of the smaller PMe_3 ligand.

For complexes **10** and **11** with the tetra-2-pyridinilpirazine ligand, the NMR experiments were registered in CD_3CN for solubility reasons. The $^{31}P\{^1H\}$ NMR spectrum of complex **10** at 235 K in CD_3CN shows two doublets due to the coupling of the phosphorus atom with the ^{107}Ag and ^{109}Ag nuclei, and two multiplets at 11.0 and 8.1 ppm with $\Delta\nu = 480$ Hz that could be assigned to the bis(phosphine)silver complex $[Ag(PPh_3)_2]^{2+}$ (Figure S3). This equilibrium between Ag(I)-monophosphine and bisphosphine derivatives has been previously observed in other silver complexes.[15c,23] In contrast, the spectrum of complex **11** at 235 K shows a broader resonance than the signal displayed at room temperature, which indicates that it is close to the coalescence temperature, but it is not possible to decrease the temperature below 235 K or to perform the NMR in CD_2Cl_2 for solubility reasons.

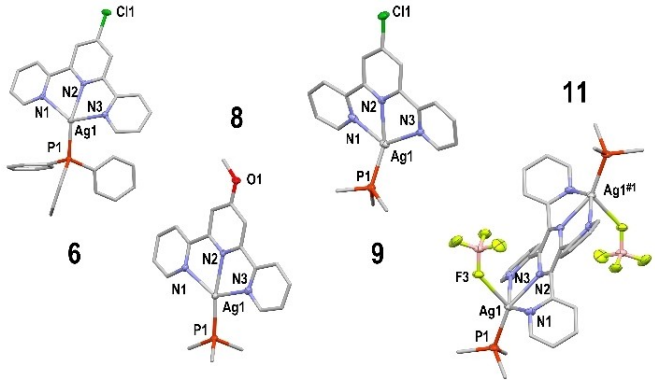

Figure 2. Crystal structure of the molecular cation in **6**, **8** and **9** and molecular structure of **11**. Hydrogen atoms have been omitted for clarity. #1 −x+2, −y, −z.

Structural Characterization

The crystal structures of complexes **6**, **8**, **9**, and **11** have been established by single crystal X-ray diffraction methods. The structures of compounds **6**, **8**, and **9** were found to be very similar, consisting of BF_4^- anions and tetracoordinated silver(I) cations in which the 4′-X-terpyridine acts as tridentate chelating ligand. The Ag^I core completes its coordination sphere by bonding to the phosphorus of a PR_3 ligand; hence, the silver coordination environment shows a highly distorted square planar geometry in the three cases, mainly due to the rigidity of the tridentate ligand (see Figure 2 and Table 1).

In the case of the dinuclear complex **11**, the presence of the hexadentate ligand tetra-2-pyridinylpyrazine allows its coordination to two silver(I) centres, whose coordination sphere is completed with the phosphorus of a trimethylphosphine ligand and one of the fluorine atoms of a tetrafluoroborate anion, as shown in Figure 2. Therefore, each silver centre in the crystal structure of **11** is pentacoordinated and displays a distorted square-based pyramidal coordination environment with the phosphorus atom occupying the apical position of the pyramid.

Stability Essays

In order to test these compounds as antitumor agents, the first step is to measure the stability of the complexes in solution and especially in biological media. The studies of the solution stability of the complexes were carried out using two different techniques: ^1H NMR and UV–Vis spectroscopies.

First, we determined the stability of the compounds comparing the ^1H NMR spectra registered in DMSO-d6 at 0 h, 8 h and 24 h (see Supporting Information Figures S5–S20). The ^1H NMR spectra showed that all the compounds remained unchanged over the whole period of 24 h, which suggests that the DMSO solvent does not influence the stability of the compounds.

In addition, the stability of the compounds was studied by monitoring the UV–Vis spectra in PBS and DMSO (20%) at different times to know how the biological environment affects the stability of the compounds. The solution of complexes was incubated at 310 K and we carried out the measurements at 0 h, 8 h and 24 h. It can be observed that there are not any

Table 1. Selected bond distances (Å) and angles (°) for complexes **6**, **8**, **9** and **11**.

Distances [Å] and angles [°]	6 Monoclinic $P2_1/a$	8 Monoclinic Cc	9 Monoclinic $P2_1/n$	11 Triclinic P-1
Ag(1)-N(1)	2.419(2)	2.439(9)	2.529(4)	2.591(9)
Ag(1)-N(2)	2.348(2)	2.391(8)	2.363(3)	2.361(8)
Ag(1)-N(3)	2.509(2)	2.452(10)	2.400(3)	2.480(8)
Ag(1)-P(1)	2.3885(7)	2.381(3)	2.3650(10)	2.365(3)
Ag(1)-F(3)	–	–	–	2.596(11)
N(1)-Ag(1)-N(2)	68.91(8)	67.5(3)	66.83(11)	68.1(3)
N(2)-Ag(1)-N(3)	67.93(7)	67.3(3)	69.26(11)	69.0(3)
N(1)-Ag(1)-P(1)	116.37(6)	118.3(2)	106.35(8)	109.4(2)
N(3)-Ag(1)-P(1)	109.05(6)	107.4(2)	120.53(8)	110.9(2)
N(2)-Ag(1)-P(1)	156.69(5)	170.9(2)	156.88(8)	155.6(2)

changes in the absorption spectra. Figure 3 shows the absorption spectra of complex **8** and those of the rest of complexes can be seen in the Supporting Information (Figures S21–S31). The data suggest that the water/DMSO (buffer PBS pH = 7.4) mixture do not influence the stabilities of the compounds.

Cytotoxic Studies

The in vitro cytotoxic activity of the silver complexes was tested against three tumour human cell lines, A549 (lung cancer), HeLa (cervix epithelial carcinoma), Jurkat (T-cell leukaemia) and one healthy cell line (lymphocytes T). Compounds are not soluble in water, but they are soluble in DMSO and in the DMSO/water mixtures used in the cytotoxicity test, which contain a small amount of DMSO ($\leq$ 1 %).

Cells were exposed to each compound for 24 h. By using the colorimetric mitochondrial function based MTT viability assay, the IC_{50} values were calculated from dose response curves obtained by nonlinear regression analysis, and the results are shown in Table 2.

All the complexes exhibit an excellent cytotoxic activity, much higher compared to cisplatin. However, complex **11** shows a selective cytotoxicity to HeLa cells, not being active in the rest of cell lines. Analysing the results, we envisage some structure-activity relationship. The presence of different sub-

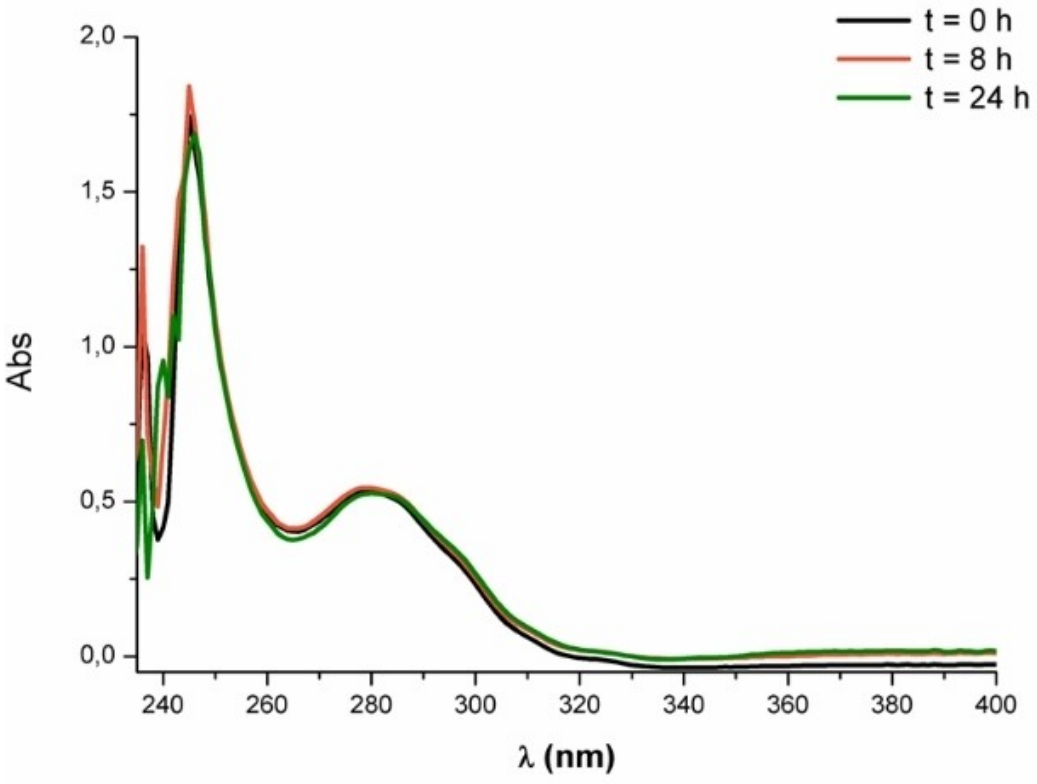

Figure 3. UV–Vis spectra for complex **8** in PBS with 20 % DMSO at 310 K.

Table 2. IC_{50} values (μM) of complexes **1**–**11** incubated for 24 h in cancer cells.

COMPLEX	A549	HeLa	Jurkat	Lymphocytes T
1	1.39 ± 0.84	3.24 ± 0.98	2.09 ± 0.40	8.46 ± 0.57
2	1.22 ± 0.88	2.95 ± 0.21	2.31 ± 0.39	6.94 ± 0.17
3	1.54 ± 0.75	3.02 ± 0.54	2.16 ± 0.12	7.5 ± 0.70
4	2.05 ± 0.47	0.76 ± 0.18	0.49 ± 0,03	0,67 ± 0,03
5	2.33 ± 0.07	0.98 ± 0.31	0.30 ± 0,06	0.39 ± 0.09
6	2.05 ± 0.13	0.85 ± 0.32	0.71 ± 0.09	0.56 ± 0.03
7	0.93 ± 0.18	2.77 ± 0.30	1.74 ± 0,48	8.02 ± 2.90
8	0.87 ± 0.29	2.90 ± 0.14	2.59 ± 0.37	8.05 ± 1.8
9	0.72 ± 0.26	2.70 ± 0.38	1.07 ± 0.13	10.89 ± 2.37
10	1.80 ± 0.31	0.67 ± 0.06	0.50 ± 0.09	0.52 ± 0,24
11	> 25	3.09 ± 0.26	> 25	> 25
Cisplatin	114.2 ± 9.1[a]	55 ± 0.9[b]	10.8 ± 0.2[a]	–

([a] at 24 h in water;[24] [b] at 24 h in DMSO[25]).

stituents in the terpyridine ligand hardly produces changes in cytotoxic activity, as can be seen in the dinuclear complexes **1**–**3**, all of which exhibit high cytotoxicity. In general, all the complexes are active, and their small differences in activity depend mainly on the ancillary ligand. Thus, the presence of a phosphine-type ligand significantly affects cytotoxicity, and the type of phosphine used also plays a role. Regarding the influence of the type of phosphine ligand employed, the compounds with PPh_3 show a slightly better activity than those with PMe_3, as indicate their IC_{50} values. Besides, while in the PPh_3-containing derivatives (**4**–**6** and **10**) the nature of the N-donor ligand hardly affects the cytotoxicity, in the case of the PMe_3 complexes (**7**–**9** and **11**) the use of tetra-2-pyridinylpyrazine instead of 4′-X-terpy (X=H, CH_3O, Cl) produces a considerable decrease in their activity (see Figure 4).

Comparison of the activity in the different tumour cells provides some interesting findings. For complexes **1**–**3**, for which ancillary ligands are not used, the most sensitive cell line is A549, whereas for HeLa and Jurkat very similar values were observed. The most interesting issue is that these compounds show selectivity against healthy cells (lymphocytes T). The selectivity index was calculated with the relation between the IC_{50} values in the Jurkat cancer cell line and the healthy lymphocytes T (see Table 3).

Compounds **4**–**6**, where the auxiliary ligand used is PPh_3, exhibit very high cytotoxicity, especially in HeLa and Jurkat cells, but they do not show selectivity towards healthy cells. The selectivity index values are close to unit, which indicates similar cytotoxicity in both cases.

Compounds **7**–**9** bearing PMe_3 as ancillary ligands also present excellent activity, especially in A549 cells, and only slightly higher values for HeLa and Jurkat cancer cells are obtained. The most interesting result is that these compounds show the highest selectivity against healthy cells (lymphocytes T), with selectivity index values of 10.2 to 3.1. In this sense, complex **9** would be the most interesting and promising complex both in terms of activity and selectivity.

The tetra-2-pyridinylpyrazine derivatives **10**–**11** show a very different behaviour each other. Thus, compound **10**, which includes PPh_3 as ancillary ligand, shows similar activity than that of compounds **7**–**9**. In contrast, compound **11** is selective for HeLa cells.

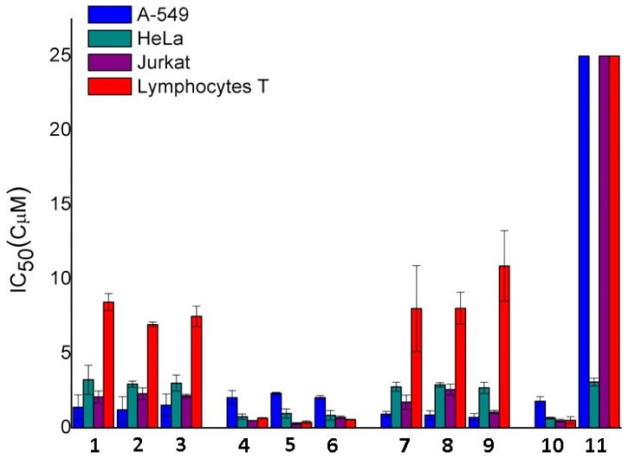

Figure 4. Representation of the IC_{50} values for complexes **1**–**11**.

DNA Binding Studies

Absorption spectral titration experiments were performed at constant concentration of the Ag(I) complexes (**1**, **4**, **7**, **10**, **11**) (20 μM) with varying concentration of the calf thymus CT-DNA (0–100 μM). The absorbance (A) of the most shifted band of the complex were recorded after successive additions of CT-DNA. A reference cell was used to nullify the absorbance due to the DNA at the measured wavelength, which contained DNA and solvent (DMSO ≤ 2% and buffer Tris HCl pH = 7.2). From the absorption titration data, the binding constant (K_b) of the Ag^I complexes with CT-DNA was determined using the Wolfe-Shimer equation:[26]

$$\frac{[DNA]}{(\varepsilon_a-\varepsilon_f)}=\frac{[DNA]}{(\varepsilon_a-\varepsilon_f)}+\frac{1}{K_b(\varepsilon_b-\varepsilon_f)} \quad (1)$$

Where ε_a corresponds to A/[Ag(I)complex], ε_f to the extinction coefficient for the free Ag^I compound and ε_b to the extinction coefficient for the silver(I) complex in the fully bound form. A plot of [DNA]/(ε_a–ε_f) versus [DNA], gives K_b as the ratio of slope to the intercept. The determined K_b values are in Table 4.

The electronic absorption spectra of the complexes on the incremental addition of CT-DNA show different behaviour depending on the ligand used, terpyridine or tetra-2-pyridinylpyrazine. In cases where the terpyridine ligand was used independently of the auxiliary ligand (**1**, **4** and **7**), there are two different regions (see Figure 5 and Figures S32–S34). In the high energy range, a hypochromic effect was observed and the absorption band decreases in intensity by the gradual addition of CT-DNA. By recording the changes in the absorbance at the chosen λ and employing the Wolfe-Shimmer equation, the quantitative DNA-binding constant K_b was calculated. Comparing this value with classical intercalators (EB K_b $1{,}4\times10^6$ M^{-1})[27] and other DNA intercalating agents in the literature,[27] it could be concluded that the complexes **4** and **7** could bind to DNA by a moderate intercalation mode. Unfortunately, for the case of compound **1** it has not been possible to calculate this constant since the response is not linear (see Supporting Information S32a/b–S34a/b). In contrast, in the low energy range of the spectrum, the intensity of the band at 335 nm

Table 4. DNA binding constants.

Complex	λ_{study} [nm]	K_b	Isosbestic Point [nm]	λ_{study} [nm]	K_b [M^{-1}]
1	290	–	313	335	–
4	277	5.34×10^4	313	335	8.05×10^3
7	290	5.08×10^4	313	335	3.50×10^3
10	265	2.98×10^5	–	–	–
11	320	2.54×10^4	–	–	–

Table 3. Selectivity index of complexes **1**–**10** in Jurkat/lymphocytes T.

COMPLEX	Jurkat	Lymphocytes T	SI
1	2.09 ± 0.40	8.46 ± 0.57	4.0
2	2.31 ± 0.39	6.94 ± 0.17	3.0
3	2.16 ± 0.12	7.5 ± 0.70	3.5
4	0.49 ± 0.03	0.67 ± 0.03	1.4
5	0.30 ± 0,06	0.39 ± 0.09	1.3
6	0.71 ± 0.09	0.56 ± 0.03	0.8
7	1.74 ± 0.48	8.02 ± 2.90	4.6
8	2.59 ± 0.37	8.05 ± 1.8	3.1
9	1.07 ± 0.13	10.89 ± 2.37	10.2
10	0.50 ± 0.09	0.52 ± 0.24	1.0

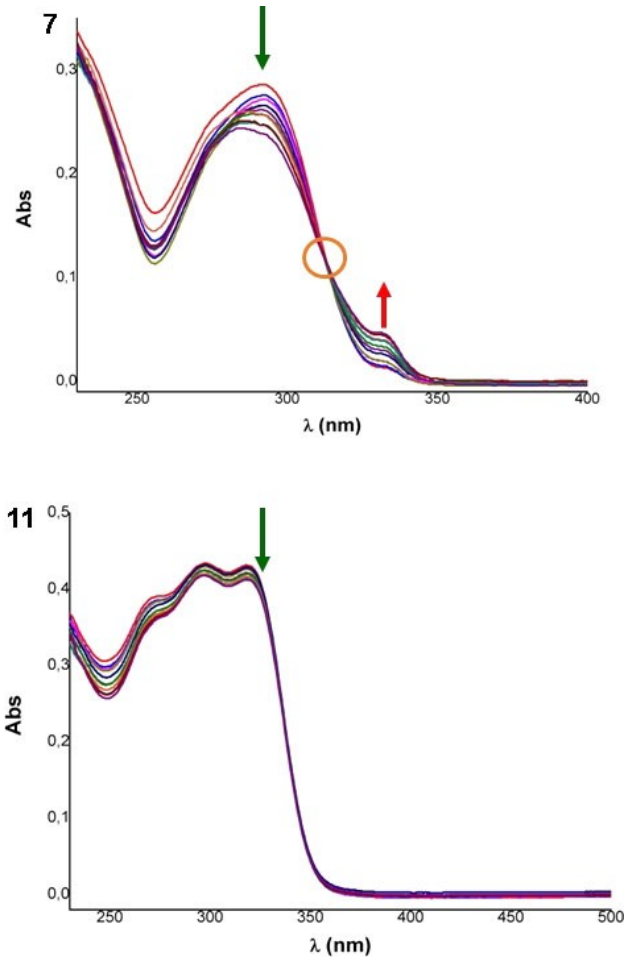

Figure 5. Absorption spectral titration experiments for complexes **7** and **11**. The green arrows indicate that the absorbance of the complex decreases and the red arrow indicates that it increases with the addition of CT-DNA. The circle marks the isosbestic point.

increases, which could be indicative of the formation of new species by electrostatic interactions between the cationic complex and the anionic phosphate groups present in the outer of the double helix of DNA. The values of DNA binding constant (K_b) are in the order of 10^3 M^{-1}, which is in accordance with a weak and unspecific electrostatic interaction.[29] Due to this dual behaviour it is possible to observe the appearance of an isosbestic point at 313 nm. This point indicates the presence of two species in equilibrium, the free complex and the complex linked to the DNA.

In the case of compounds **10** and **11**, where the ligand used is tetra-2-pyridinylpyrazine, only one type of behaviour was observed (see Figure 5 and supporting Information S35–S36). The intensity of the band decreases as the CT-DNA concentration increases, which could indicate that the interaction occurs through an intercalation mode. As in the previous cases, the quantitative DNA binding constant K_b is calculated. Comparing these values with classical intercalators (EB K_b $1{,}4 \times 10^6$ M^{-1})[27] and other DNA intercalative agents in the literature,[28] it could be concluded that complexes **10** and **11** could bind to DNA by a moderate intercalation mode (see S30a–S31a).

Cell Death Study

A characteristic feature of cancer cells is that a disruption of the balance between dividing cells and cell death exists. Besides, the progression of this disease is based on the dysregulation of cell death pathways. Consequently, it is important to know the mechanism through which the complexes are capable of inducing cell death, being of particular interest compounds able to induce a programmed cell death mechanism such as apoptosis. Cell death mechanism was analysed by flow cytometry and, for that purpose, Jurkat and Jurkat shBak (apoptosis-resistant cell line via mitochondrial pathway) were used. Compounds $[Ag(PPh_3)(terpy)]BF_4$ (**4**) and $[Ag(PMe_3)(terpy)]BF_4$ (**7**) were selected for this purpose. We selected these compounds because both are quite active against Jurkat cell line and show large differences in selectivity index (**4** SI = 1.4 and **7** SI = 4.6). Cells were incubated 24 h in the presence of 10 μM of the corresponding compounds **4** or **7** and anexin V-DY634 (anexin binds phosphatidylserine on the external surface of apoptotic cells). As shown in Figure 6, the number of apoptotic cells is much higher in Jurkat cell line than in Jurkat shBak with 82.3% (**4**) and 60.2% (**7**) and 41.7% (**4**) y un 23.2% (**7**) of apoptotic cells, respectively. These results suggest that these derivatives induce cell death via mitochondrial pathway. To evaluate better this effect, the same procedure was carried out at different concentrations. As illustrated in Figure 6 (bottom), percentage of apoptotic cells was higher as complex concentrations increased. Intriguingly, lower percentage of apoptotic cells was always observed in Jurkat shBak cell line.

In order to confirm that the compounds effectively induce cell death by a mechanism of apoptosis, an assay was carried out with Jurkat cells in the presence and absence of z-VAD (pan-caspase inhibitor). Therefore, in the presence of this inhibitor (z-VAD), a strong decrease in the number of apoptotic cells was observed (**4**) 93.4% vs 35.9% and (**7**) 71.9% vs 22.5% (see Figure 7). Therefore, considering that caspases are a family of enzymes that initiate and execute apoptosis, it seems confirmed that these compounds induce this type of cell death. The measurements were carried out at different concentrations (see Figure 7 bottom).

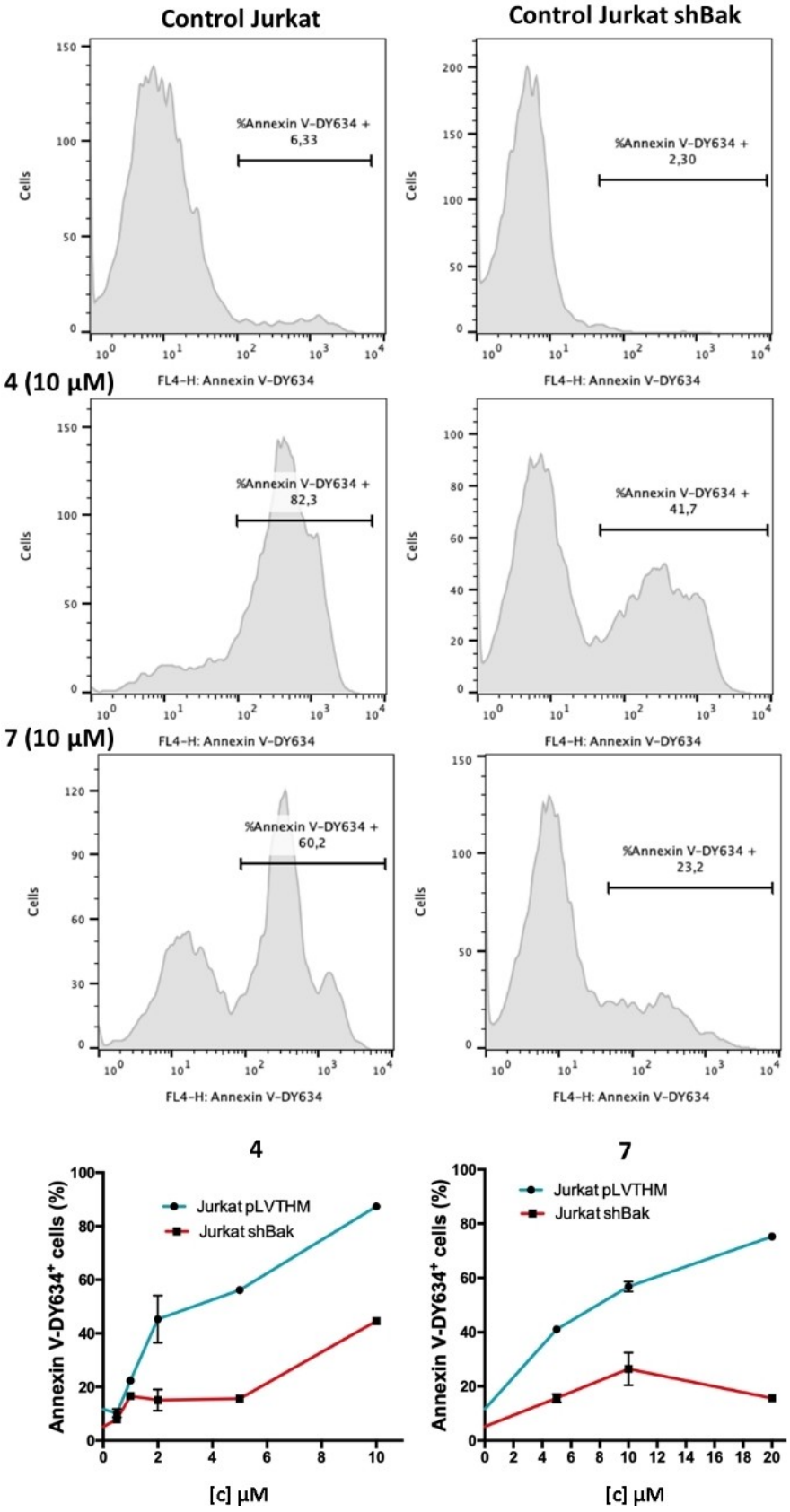

Figure 6. Flow cytometry for complex **4** and **7** in Jurkat and Jurkat shBak.

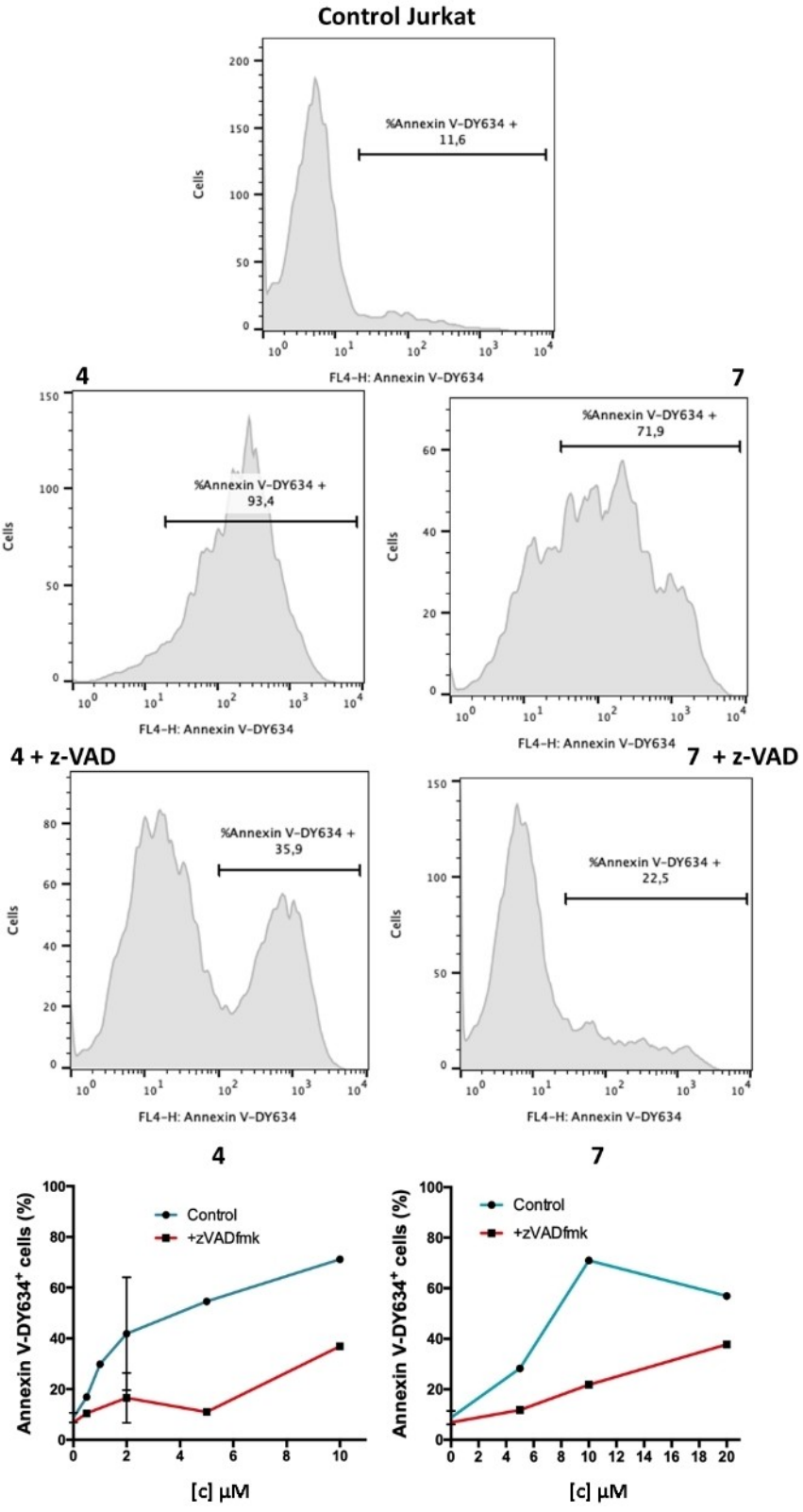

Figure 7. Flow cytometry for compounds **4** and **7** incubated in Jurkat with and without z-VAD.

Conclusions

The synthesis and study of antitumor properties of a family of silver derivatives using nitrogen donor ligands such as 4-substituted terpyridines and tetra-2-pyridinylpyrazine, as well as the use or not of phosphines as ancillary ligands, has been carried out. Dinuclear complexes **1**–**3** with the general formula $[Ag(S)(4'\text{-X-terpyridine})]BF_4$, or complexes with phosphines as ancillary ligands and the different 4′-X-terpyridine or tetra-2-pyridinylpyrazine ligands were synthesised affording complexes with general formula $[Ag(PR_3)(4'\text{-X-terpyridine})]BF_4$ (**4**–**9**) and $[Ag_2(PR_3)_2(\text{tetra-2-pyridinylpyrazine})](BF_4)_2$ (**10**–**11**).

The study of antitumour properties revealed interesting results and a structure-activity relationship could be established. Different tumour cell lines A-549 (lung cancer), HeLa (cervix epithelial carcinoma), and Jurkat (T-cell leukaemia), as well as healthy lymphocytes T were used. All compounds were found to be active except compound **11** which only showed a selective activity against HeLa. However, different behaviours were observed. The presence of different substituents on the terpyridine ligand provided virtually no change. On the other hand, the use or not of PPh_3 or PMe_3 seems to be a key factor. Thus compounds **1**–**3** showed some selectivity against healthy cells. The presence of PPh_3 (**4**–**6**, **10**) promotes greater cytotoxicity, but no selectivity. On the contrary, the use of the PMe_3 ligand provides some selectivity against healthy lymphocytes T, compound **9** being one of the most promising compounds with a selectivity index of 10.2.

The mechanism of action of silver(I) complexes is still not completely clear, although some studies suggest that a possible mechanism of action of such compounds could be DNA binding and cleavage.[14,15] For this reason, the possible mechanism according to which these derivatives may interact with DNA has been evaluated.

The absorption spectral titration experiments have shown that the use of different phosphines is not a determining factor in this respect. However, a different behaviour was observed depending on the ligand used, terpyridine or tetra-2-pyridinylpyrazine. Thereby, compounds **1**, **4**, and **7** act as moderate intercalants and produce electrostatic interactions between the cationic complex and the anionic phosphate groups present in the DNA double helix. On the other hand, complexes **10** and **11** show only one type of behaviour, acting as moderate intercalating agents.

Finally, and as we mentioned above, tumour cells disrupt the balance between proliferation and death. In this sense, a study was carried out to determine the mechanism in which these derivatives induce cell death. Compounds **4** and **7** were selected for this purpose and it was concluded that both derivatives were capable of inducing cell death through a mechanism that activates the mitochondrial apoptotic pathway.

Therefore, we infer that these results corroborate the great potential of silver derivatives for the future development of new anticancer agents.

Experimental Section

Experimental Details: Fourier transform infrared (FT-IR) spectra were recorded in the 4000–450 cm^{-1} range on a PerkinElmer μ-ATR Spectrum II. C, H, and N analyses were carried out with PerkinElmer 240 C microanalyzer. Bruker Microflex matrix-assisted laser desorption ionization time-of-flight mass spectrometer (MALDI-TOF MS) using 11-dicyano-4-tert-butylphenyl-3-methylbutadiene (DCTB) as matrix. ^1H and $^{31}P\{^1H\}$ NMR spectra were recorded with a Bruker Avance 400 spectrometer in CD_2Cl_2, DMSO-d6 and CD_3CN. Absorption spectra in solution were recorded on a Hewlett-Packard 8453 diode array UV–Vis spectrophotometer.

Materials and Procedures: 2,2′:6′2″-terpyridine, tetra-2-pyridinylpyrazine, 4′-Cl-2,2′:6′2″-terpyridine, $AgBF_4$, $P(CH_3)_3$ and PPh_3 were purchased from Alfa Aesar or Sigma Aldrich and used as received. 4′-CH_3O-terpyridine was prepared according to the literature.[30]

Synthesis of $[Ag(S)(PPh_3]BF_4$: To a solution of $AgBF_4$ (m = 1.0657 g, n = 5.47 mmol) in 40 mL of THF was added 1 equivalent of PPh_3 (m = 1.4348 g, n = 5.47 mmol) and the reaction mixture was stirred during 1 h, and then concentrated under vacuum. The $[(S)AgPPh_3]BF_4$ complex was precipitated with diethyl ether, and a white solid was obtained, yield 85 % (m = 2.1247 g, n = 4.64 mmol). ^1H NMR (400 MHz, CD_2Cl_2, ppm) δ 7.57–7.44 (m, 15H). $^{31}P\{H\}$ NMR (162 MHz, CD_2Cl_2, ppm) δ 16.91 (m, 1P). ^1H NMR (400 MHz, CD_2Cl_2, ppm 220 K) δ 7.58–7.36 (m, 15H). $^{31}P\{^1H\}$ NMR (162 MHz, CD_2Cl_2, ppm 220 K) δ 18.59–13.22 (2 d, 1P, $AgPPh_3$, $J_{109\ Ag\text{-}P}$ = 868.38 Hz, $J_{107\ Ag\text{-}P}$ = 752.85 Hz), δ 16.68–13.06 (2 d, 2P, $Ag(PPh_3)_2$, $J_{109\ Ag\text{-}P}$ = 584.77 Hz, $J_{107\ Ag\text{-}P} \approx 509$ Hz).

Synthesis of $[Ag(4'\text{-X-terpyridine})]BF_4$ (X=H (1), CH_3O (2), Cl (3)): To a solution of $AgBF_4$ (m = 0.100 g, n = 0.51 mmol) in 20 mL of diethyl ether was added 1 equivalent of 4′-X-terpyridine (X=H m = 0.1189 g, X=CH_3O m = 0.1342 g, X=Cl m = 0.1365 g), immediately appear a white solid and the reaction mixture was stirred during 2 h, finally the solid was filtrated ([4′-X-terpyridine-Ag]BF_4 (X=H **1**, CH_3O **2**, Cl **3**).

Complex 1 $[Ag(terpyridine)]BF_4$: Yield 88 %, white solid (m = 0.1920 n = 0.45 mmol). ^1H NMR (400 MHz, DMSO-d6, ppm) δ 8.63 (m, 2H, H_1), δ 8.52–8.50 (m, 4H, $H_5 + {}_{H4)}$, δ 8.28 (m, 2H, H6), δ 8.09 (ddd, 2H, H_3, $_{3JH3\text{-}H2} \sim {}^3J_{H3\text{-}H4}$ = 7.77 Hz, $^4J_{H3\text{-}H1}$ = 1.61 Hz), δ 7.60 (m, 2H, H_2). MALDI-TOF(+) *m/z*: $[Ag(terpy)]^+$ = 340; $[Ag(terpy)_2]^+$ = 573; MALDI-TOF(−) *m/z*: $[BF_4]^-$ = 87. FTIR: ν(C=N) at 1598–1564 cm^{-1}; ν (C=C) 1478 cm^{-1}; ν (CAr–H) vibration bending 1049–993 cm^{-1}. Analytical data (%): $C_{15}H_{11}AgBF_4N_3$ (427.40) requires 42.10 % C; 2.59 % H; 9.82 % N. Found: 42.43 % C; 2.21 % H; 10.14 % N.

Complex 2 $[Ag(4'\text{-}CH_3O\text{-terpyridine})]BF_4$: Yield 86 %, white solid (m = 0.2008 n = 0.44 mmol). ^1H NMR (400 MHz, DMSO-d6, ppm) δ 8.58 (m, 2H, H1), δ 8.49 (d, 2H,H4, $^3J_{H4\text{-}H3}$ = 7.48 Hz), δ 8.09 (ddd, 2H, H3, $^3J_{H3\text{-}H2} \sim {}^3J_{H3\text{-}H4}$ = 7.86 Hz, $^4J_{H3\text{-}H1}$ = 1.52 Hz), δ 8.02 (s, 2H, H5) δ 7.59 (m, 2H, H_2), δ 4.10 (s, 3H, CH_3O). MALDI-TOF(+) *m/z*: $[Ag(4'\text{-}CH_3O\text{-terpy})]^+$ = 370; $[Ag(4'\text{-}CH_3O\text{-terpy})_2]^+$ = 633; MALDI-TOF(−) *m/z*: BF_4^- = 87. FTIR: ν(C=N) at 1596–1563 cm^{-1}; ν(C=C) 1479 cm^{-1}; ν(Ar–O) 1361 cm^{-1}; ν(C–O) 1227 cm^{-1}; $\nu(C^{Ar}\text{–}H)$ vibration bending 1049–992 cm^{-1}. Analytical data (%): $C_{16}H_{13}AgBF_4N_3O$ (457.83) requires 41.96 % C; 2.86 % H; 9.18 % N. Found: 42.18 % C; 2.99 % H; 9.36 % N.

Complex 3 $[Ag(4'\text{-Cl-terpyridine})]BF_4$: Yield 90 %, white solid (m = 0.2122 n = 0.46 mmol). ^1H NMR (400 MHz, DMSO-d6, ppm) δ 8.67 (m, 2H, H1), δ 8.63 (s, 2H, H5), δ 8.56 (m, 2H, H4), δ 8.11 (m, 2H, H3, $^3J_{H3\text{-}H2} \sim {}^3J_{H3\text{-}H4}$ = 7.88 Hz, $^4J_{H3\text{-}H1}$ = 1.60 Hz), δ 7.63 (m, 2H, H2). MALDI-TOF(+) *m/z*: $[Ag(4'\text{-Cl-terpy})]^+$ = 376; $[(Ag(4'\text{-Cl-terpy})_2]^+$ = 643; MALDI-TOF(−) *m/z*: BF_4^- = 87. FTIR: ν(C=N) at 1598–1556 cm^{-1}; ν(C=C) 1479 cm^{-1}; $\nu(C^{Ar}\text{–}H)$ vibration bending 1049–993 cm^{-1}.

Analytical data (%): $C_{15}H_{10}AgBClF_4N_3$ (462.28) requires 38.96% C; 2.18% H; 9.09% N. Found: 38.74% C; 2.22% H; 9.16% N.

Synthesis of [Ag(PPh_3)(4′-X-terpyridine)]BF_4 (X=H 4, CH_3O 5, Cl 6): To a solution of [AgPPh_3]BF_4 (m = 0.100 g, n = 0,22 mmol) in 20 mL CH_2Cl_2 was added 1 equivalent of 4′-X-terpyridine n = 0.22 mmol (X=H m = 0.0509 g, X=CH_3O m = 0.0518 g, X=Cl m = 0.0609 g), stirred the mixture during 2 h and reduced the volume under vacuum. The complex [Ag(PPh_3)(4′-X-terpyridine)]BF_4 (X=H **4**, CH_3O **5**, Cl **6**) was precipitated with diethyl ether.

Complex 4 [Ag(PPh_3)(terpyridine)]BF_4: Yield 85%, white solid (m = 0.1291 n = 0.19 mmol). ^{1}H NMR (400 MHz, CD_2Cl_2, ppm) δ 8.31–8.26 (m, 5H, $H_4+H_5+H_6$), δ 8.17 (m, 2H, H_1), δ 8.00 (m, 2H, H_3), δ 7.53 (m, 3H, H_2 + 1H–Ph), δ 7.45–7.41 (m, 6H, Ph), δ 7.38–7.33 (m, 8H, Ph). ^{31}P{^{1}H} NMR (162 MHz, CD_2Cl_2, ppm) δ 14.43–10.66 (m, 1P). ^{31}P {^{1}H} NMR (162 MHz, CD_2Cl_2, ppm 220 K) δ 13.98–9.57 (2 d, 1P, $J_{109\ Ag\text{-}P}$ = 715.04 Hz, $J_{107\ Ag\text{-}P}$ = 620.34 Hz). MALDI-TOF(+) *m/z*: [Ag(PPh_3)(terpy)]$^+$ = 602; [Ag(terpy)$_2$]$^+$ = 573; [Ag(PPh_3)$_2$]$^+$ = 631; MALDI-TOF(−) *m/z*: [BF_4]$^-$ = 87. N. FTIR: ν(C=N) at 1590–1571 cm^{-1}; ν(C=C) 1480–1471 cm^{-1}; ν(C^{Ar}–H) vibration bending 1048–1035 cm^{-1}; ν(P–C) stretch 707–693 cm^{-1}. Analytical data (%): $C_{33}H_{26}AgBF_4N_3P$ (690.22) requires 57.42% C; 3.80% H; 6.09% N. Found: 57.78% C; 3.91% H; 6.14% N.

Complex 5 [Ag(PPh_3)(4′-CH_3O-terpyridine)]BF_4: Yield 71%, white solid (m = 0.1127 n = 0.16 mmol). ^{1}H NMR (400 MHz, CD_2Cl_2, ppm) δ 8.24 (d, 2H, H4, $^3J_{H4\text{-}H3}$ = 7.86 Hz), δ 8.16 (m, 2H, H1), δ 7.97 (ddd, 2H, H_3, $^3J_{H3\text{-}H2} \sim {}^3J_{H3\text{-}H4}$ = 7.85 Hz, $^4J_{H3\text{-}H1}$ = 1.55 Hz), δ 7.75 (s, 2H, H5), δ 7.55–7.51 (m, 3H, H_2 + 1H–Ph), δ 7.45–7.41 (m, 6H, Ph), δ 7.36–7.31 (m, 8H, Ph), δ 4.15 (s, 3H, CH_3O). ^{31}P{H} NMR (162 MHz, [D_2]-CD_2Cl_2, ppm) δ 15,23–11,54 (m, 1P). ^{1}H NMR (400 MHz. ^{31}P{^{1}H} NMR (162 MHz, CD_2Cl_2, ppm 220 K) δ 14.51–10.07 (2 d, 1P, $J_{109\ Ag\text{-}P}$ = 718.94 Hz, $J_{107\ Ag\text{-}P}$ = 624.64 Hz). MALDI-TOF(+) *m/z*: [Ag(PPh_3)(4′-CH_3O-terpyridine)]$^+$ = 632; [Ag(4′-CH_3O-terpy)]$^+$ = 370. MALDI-TOF(−) *m/z*: [BF_4]$^-$ = 87. N. FTIR: ν(C=N) at 1595–1558 cm^{-1}; ν(C=C) 1477 cm^{-1}; ν(Ar–O) 1361 cm^{-1}; ν(C–O) 1227 cm^{-1}; ν(C^{Ar}-H) vibration bending 1058–1031 cm^{-1}; ν(P–C) stretch 707–692 cm^{-1}. Analytical data (%): $C_{34}H_{28}AgBF_4N_3OP$ (720.25) requires 56.70% C; 3.92% H; 5.83% N. Found: 56.86% C; 4.01% H; 5.93% N.

Complex 6 [Ag(PPh_3)(4′-Cl-terpyridine)]BF_4: Yield 79%, yellow solid (m = 0.1261 n = 0.17 mmol). ^{1}H NMR (400 MHz, CD_2Cl_2, ppm) δ 8.28 (s, 2H, H5), δ 8.24 (d, 2H, H4, $^3J_{H4\text{-}H3}$ = 7,85 Hz), δ 8.20 (m, 2H, H1), δ 8.01 (ddd, 2H, H3, $^3J_{H3\text{-}H2} \sim {}^3J_{H3\text{-}H4}$ = 7.75 Hz, $^4J_{H3\text{-}H1}$ = 1.65 Hz), δ 7.0, Ph). ^{31}P{^{1}H} NMR (162 MHz, CD_2Cl_2, ppm) δ 14.98–10.79 (m, 1P). ^{31}P {^{1}H} NMR (162 MHz, CD_2Cl_2, ppm 220 K) δ 14.51–10.07 (2 d, 1P, $J_{109\ Ag\text{-}P}$ = 719,52 Hz, $J_{107\ Ag\text{-}P}$ = 623,73 Hz). MALDI-TOF(+) *m/z*: [Ag(PPh_3)(4′-Cl-terpyridine)]$^+$ = 638; [Ag(4′-Cl-terpy)]$^+$ = 376; [Ag(PPh_3)$_2$]$^+$ = 631. MALDI-TOF(−) *m/z*: [BF_4]$^-$ = 87. FTIR: ν(C=N) at 1582–1554 cm^{-1}; ν(C=C) 1478–1472 cm^{-1}; ν(C^{Ar}–H) vibration bending 1057–1025 cm^{-1}; ν(P–C) stretch 705–694 cm^{-1}. Analytical data (%): $C_{33}H_{25}AgBClF_4N_3P$ (724.67) requires 54.69% C; 3.48% H; 5.80% N. Found: 54.48% C; 3.62% H; 5.73% N.

Synthesis of [Ag($P(CH_3)_3$)(4′-X-terpyridine)]BF_4 (X = H 7, CH_3O 8, Cl 9): Under argon atmosphere. To a solution of 0.36 mL of $P(CH_3)_3$ (0.36 mmol) in dry CH_2Cl_2 (20 mL) was added 0.0708 g (0.36 mmol) of $AgBF_4$ and the reaction mixture was stirred for 1 h. After this period was added 1 equivalent of 4′-X-terpyridine (X=H m = 0.0839 g, X=CH_3O m = 0.0947 g, X=Cl m = 0.0964 g). After stirring the mixture during 2 h and reducing the volume under vacuum, the complex was precipitated with diethyl ether on air to give [Ag($P(CH_3)_3$)(4′-X-terpyridine)]BF_4 (X = H **7**, CH_3O **8**, Cl **9**).

Complex 7 [Ag($P(CH_3)_3$)(terpyridine)]BF_4: Yield 75%, yellow solid (m = 0.1360 n = 0.27 mmol). ^{1}H NMR (400 MHz, CD_2Cl_2, ppm) δ 8.72 (m, 2H, H1), δ 8.27-8.23 (m, 5H, H6 + H5 + H4), δ 8.07 (ddd, 2H, H3, $^3J_{H3\text{-}H2} \sim {}^3J_{H3\text{-}H4}$ = 7.76 Hz, $^4J_{H3\text{-}H1}$ = 1.66 Hz), δ 7.61 (ddd, 2H, H2, $^3J_{H2\text{-}H3}$ = 7,43 Hz, $^3J_{H2\text{-}H1}$ = 5,02 Hz, $^4J_{H2\text{-}H4}$ = 0,67 Hz), δ 1.41 (m, 9H, P–$(CH_3)_3$). ^{31}P{^{1}H} NMR (162 MHz, CD_2Cl_2, ppm) δ −37.04 (m, 1P). ^{31}P {^{1}H} NMR (162 MHz, CD_2Cl_2, ppm 190 K) δ (−36.03)–(−40.29) (d, 1P, Δν = 705 Hz). MALDI-TOF(+) *m/z*: [Ag($P(CH_3)_3$)(terpy)]$^+$ = 416; [Ag(terpy)]$^+$ = 340; [Ag(terpy)$_2$]$^+$ = 573; MALDI-TOF(−) *m/z*: [BF_4]$^-$ = 87. FTIR: ν(C=N) at 1589–1570 cm^{-1}; ν(C=C) 1473 cm^{-1}; ν(C^{Ar}–H) vibration bending 1047–1034 cm^{-1}; ν(P–CH_3) rocking 954 cm^{-1}. Analytical data (%): $C_{18}H_{20}AgBF_4N_3P$ (503.84) requires 42.89% C; 4.00% H; 8.34% N. Found: 43.04% C; 4.35% H; 8.54% N.

Complex 8 [Ag($P(CH_3)_3$)(4′-CH_3O-terpyridine)]BF_4: Yield 81%, white solid (m = 0.1557 n = 0.29 mmol). ^{1}H NMR (400 MHz, CD_2Cl_2, ppm) δ 8.65 (m, 2H, H1), δ 8.20 (d, 2H, H4, $^3J_{H4\text{-}H3}$ = 7.42 Hz), δ 8.06 (ddd, 2H, H3, $^3J_{H3\text{-}H2} \sim {}^3J_{H3\text{-}H4}$ = 7.70 Hz, $^4J_{H3\text{-}H1}$ = 1.53 Hz), δ 7.66 (m, 2H, H5), δ 7.58 (m, 2H, H2), δ 4.13 (s, 3H, CH_3O), δ 1.31 (m, 9H, P–$(CH_3)_3$). ^{31}P{^{1}H} NMR (162 MHz, CD_2Cl_2, ppm) δ −37.15 (m, 1P). ^{31}P {^{1}H} NMR (162 MHz, CD_2Cl_2, ppm 190 K) δ (−34.95)–(−39.34) (d, 1P, Δν = 734 Hz). MALDI-TOF(+) *m/z*: [Ag($P(CH_3)_3$)(4′-CH_3O-terpyridine)]$^+$ = 446; [Ag(4′-CH_3O-terpy)]$^+$ = 370; [Ag(4′-CH_3O-terpy)$_2$]$^+$ = 633; MALDI-TOF(−) *m/z*: [BF_4]$^-$ = 87. FTIR: ν(C=N) at 1686–1558 cm^{-1}; ν(C=C) 1475 cm^{-1}; ν(Ar–O) 1361 cm^{-1}; ν(C–O) 1222 cm^{-1}; ν(C^{Ar}–H) vibration bending 1045–1029 cm^{-1}; ν(P–CH_3) rocking 951 cm^{-1}. Analytical data (%): $C_{19}H_{22}AgBF_4N_3OP$ (533.84) requires 42.73% C; 4.15% H; 7.87% N. Found: 42.94 C; 4.44% H; 7.99% N.

Complex 9 [Ag($P(CH_3)_3$)(4′-Cl-terpyridine)]BF_4: Yield 77%, yellow solid (m = 0.1432 n = 0.28 mmol). ^{1}H NMR (400 MHz, CD_2Cl_2, ppm) δ 8.67 (m, 2H, H1), δ 8.21–8.19 (m, 4H, H5 + H4), δ 8.06 (ddd, 2H, H3, $^3J_{H3\text{-}H2} \sim {}^3J_{H3\text{-}H4}$ = 7.83 Hz, $^4J_{H3\text{-}H1}$ = 1.56 Hz), δ 7.61 (m, 2H, H2), δ 1.37 (m, 9H, P–$(CH_3)_3$). ^{31}P{^{1}H} NMR (162 MHz, CD_2Cl_2, ppm) δ −39.16 (m, 1P). ^{31}P{^{1}H} NMR (162 MHz, CD_2Cl_2, ppm 190 K) δ (−36.53)–(−41.29) (2 d, 1P, $J_{109\ Ag\text{-}P}$ = 771.43 Hz, $J_{107\ Ag\text{-}P}$ = 661.09 Hz). MALDI-TOF(+) *m/z*: [Ag($P(CH_3)_3$)(4′-Cl-terpyridine)]$^+$ = 452; [Ag(4′-Cl-terpy)]$^+$ = 376; [Ag(4′-Cl-terpy)$_2$]$^+$ = 643; MALDI-TOF(−) *m/z*: BF_4^- = 87. FTIR: ν(C=N) at 1582–1559 cm^{-1}; ν(C=C) 1471 cm^{-1}; ν(C^{Ar}–H) vibration bending 1049–1035 cm^{-1}; ν(P–CH_3) rocking 970–957 cm^{-1}. Analytical data (%): $C_{18}H_{19}AgBClF_4N_3P$ (538.29) requires 40.15% C; 3.56% H; 7.80% N. Found: 40.36% C; 3.82% H; 7.97% N.

Synthesis of [Ag_2(PPh_3)$_2$(tetra-2-pyridinylpyrazine)]$(BF_4)_2$ 10: To a solution of [AgPPh_3]BF_4 (m = 0.0816 g, n = 0.18 mmol) in 20 mL CH_2Cl_2 and was added 0.5 equivalent of tetra-2-pyridinylpyrazine (m = 0.0349 g, n = 0.09 mmol) and the mixture stirred during 2 h and reduced the volume under vacuum. The complex was precipitated with diethyl ether as an yellow solid. Yield: 79% (m = 0.1852 g, n = 0.14 mmol). ^{1}H NMR (400 MHz, CD_3CN, ppm) δ 8.37 (m, 4H, H1), δ 7.76 (ddd, 4H, H3, $^3J_{H3\text{-}H2} \sim {}^3J_{H3\text{-}H4}$ = 7.98 Hz, $^4J_{H3\text{-}H1}$ = 1.49 Hz), δ 7.68 (d, 4H, H4, $^3J_{H4\text{-}H3}$ = 7.93 Hz), δ 7.50 (m, 6H, Ph), δ 7.41 (m,12H, Ph), δ 7.36 (m, 4H, H2), δ 7.28 (m,12H, Ph). ^{31}P{^{1}H} NMR (162 MHz, CD_3CN, ppm) δ 10.70 (m, 2P, ^{31}P{^{1}H} NMR (162 MHz, CD_3CN, ppm 235 K) δ 12.81–8.52 (2 d, 2P, 2 Ag-PPh_3, $J_{109\ Ag\text{-}P}$ = 707.17 Hz, $J_{107\ Ag\text{-}P}$ = 602.31 Hz) δ 11.03–8.06 (m, 4P, 2 Ag(PPh_3)$_2$, Δν = 480 Hz). MALDI-TOF(+) *m/z*: [Ag(PPh_3)(tetra-2-pyridinylpyrazine)]$^+$ = 757; [Ag(tetra-2-pyridinylpyrazine)]$^+$ = 495 [Ag(tetra-2-pyridinylpyrazine)$_2$]$^+$ = 883; [Ag(PPh_3)$_2$]$^+$ = 631; MALDI-TOF(−) *m/z*: BF_4^- = 87. FTIR: ν(C=N) at 1595–1572 cm^{-1}; ν(C=C) 1483–1475 cm^{-1}; ν(=C–H) vibration bending 1050–1034 cm^{-1}; ν(P–C) stretch 692 cm^{-1}. Analytical data (%): $C_{60}H_{46}Ag_2B_2F_8N_6P_2$ (1302.34) requires 55.33% C; 3.56% H; 6.45% N. Found: 55.01% C; 3.78% H; 6.77% N.

Synthesis of [Ag_2($P(CH_3)_3$)$_2$(tetra-2-pyridinylpyrazine)]$(BF_4)_2$ 11: To a solution under argon atmosphere of 0.41 mL of $P(CH_3)_3$ (0.41 mmol) in dry CH_2Cl_2 (20 mL) was added 0.0807 g (0.41 mmol) of $AgBF_4$ and the reaction mixture stirred for 1 h. Then, 0.5 equivalent of tetra-2-pyridinylpyrazine n = 0.20 mmol (m = 0.0796 g) was added and stirred the mixture during 2 h. Finally, concentration of

the volume under vacuum and addition of diethyl ether afforded a yellow solid of complex $[Ag_2(P(CH_3)_3)_2$(tetra-2-pyridinylpyrazine)$](BF_4)_2$. ^{1}H NMR (400 MHz, CD_3CN, ppm) δ 8.50 (m, 4H, H1), δ 7.89 (ddd, 4H, H3, $^3J_{H3\text{-}H2} \sim {}^3J_{H3\text{-}H4} = 7.88$ Hz, $^4J_{H3\text{-}H1} = 1{,}65$ Hz), δ 7.87 (d, 4H, H4, $^3J_{H4\text{-}H3} = 7.87$ Hz), δ 7.48 (m, 4H, H2), δ 1.24 (m, 18H, P-$(CH_3)_3$). ^{31}P{^{1}H} NMR (162 MHz, CD_3CN, ppm) δ −37.83 (m, 2P). ^{31}P{^{1}H} NMR (162 MHz, CD_3CN, ppm 235 K) δ (−35.28)–(−39.35) (m, 1P). MALDI-TOF(+) *m/z*: $[Ag(P(CH_3)_3)$(tetra-2-pyridinylpyrazine)$]^+ = 571$; $[Ag$-(tetra-2-pyridinylpyrazine)$]^+ = 495$; $[Ag$(tetra-2-pyridinylpyrazine)$_2]^+ = 882$; MALDI-TOF(−) *m/z*: $[BF_4]^- = 87$. FTIR: ν(C=N) at 1587–1566 cm^{-1}; ν(C=C) 1483–1475 cm^{-1}; $\nu(C^{Ar}$-H) vibration bending 1048–1035 cm^{-1}; ν(P-CH_3) rocking 962–949 cm^{-1}. Analytical data (%): $C_{30}H_{34}Ag_2B_2F_8N_6P_2$ (929.92) requires 38.75% C; 3.69% H; 9.04% N. Found: 38.98% C; 3.80% H; 9.34% N.

X-ray structure determination: Single crystals suitable for X-ray diffraction studies were obtained layering saturated dichloromethane solutions with diethyl ether at room temperature. The crystals were mounted in inert oil on glass fibres and transferred to the cold gas stream of a Nonius Kappa CCD diffractometer equipped with an Oxford Instruments low-temperature attachment. Data were collected using monochromated Mo Kα radiation ($\lambda =$ 0.71073 Å). Scan type: ω and φ. Absorption correction: semi-empirical (based on multiple scan). The structures were solved by direct methods and refined on F^2 using the program SHELXL-97.[31] All non-hydrogen atoms were refined anisotropically. Hydrogen atoms were included using a riding model. The fluorine atoms of the $[BF_4]^-$ anion in **6** and **9** as well as the methyl groups of the PMe_3 ligands in **11** were found to be disordered over two positions (70:30, 50:50 and 65:35, respectively).

Deposition Numbers 2235048 (**6**), 2235049 (**8**), 2235050 (**9**), 2235051 (**11**) contain the supplementary crystallographic data for this paper. These data are provided free of charge by the joint Cambridge Crystallographic Data Centre and Fachinformationszentrum Karlsruhe Access Structures service.

Cytotoxicity assay: The MTT assay was used to determine cell viability as an indicator for cells sensitivity to the complexes. Exponentially growing cells A549, HeLa, Jurkat and healthy lymphocytes T were seeded at a density of approximately 1×10^4 cells (A549, HeLa) or 3×10^4 cells (Jurkat, healthy lymphocytes T) per well in 96-well flat-bottomed microplates. The complexes were dissolved in DMSO and then diluted with culture medium to obtain the final concentrations ranging from 0.1 μM to 25 μM in quadruplicate. Cells were incubated with the compounds for 24 h at 37 °C. 10 μL of MTT (5 mg mL^{-1}) were added to each well and plates were incubated for 2 h at 37 °C. Then, media was discarded and DMSO (100 μL per well) was added to dissolve the formazan precipitates in the plates containing A549 and HeLa cells. Alternatively, plates containing either Jurkat and healthy lymphocytes T were previously centrifuged for 15 min at 2500 rpm. Thereafter, media was also eliminated and DMSO (100 μL per well) was added. The optical density was measured at 550 nm using a 96-well multiscanner autoreader, Multieskan EX (Thermo Scientific). The IC_{50} was calculated by nonlinear regression analysis using OriginPro.

DNA Binding: In DNA binding experiments, the complexes were dissolved in DMSO and diluted with the Tris-HCl buffer (10 mM, pH = 7.4). The absorption spectra were performed in fixed concentration of metal complexes (20 μM) while gradually increasing the concentration of CT-DNA with 0 to 100 μM. To obtain the absorption spectra, the required amount of CT-DNA was added to both compound solution and the reference solution to eliminate the absorbance of CT-DNA itself. Each sample solution was allowed to equilibrate 5 min before the spectra was recorded. Using the absorption titration data, the binding constant K_b was determined using the equation:[25]

$$\frac{[DNA]}{(\varepsilon_a-\varepsilon_f)}=\frac{[DNA]}{(\varepsilon_a-\varepsilon_f)}+\frac{1}{K_b(\varepsilon_b-\varepsilon_f)} \quad (2)$$

where [DNA] is the concentration of CT-DNA, ε_a corresponds to the extinction coefficient observed ($A_{obsd}/[M]$), ε_f corresponds to coefficient of free compound, ε_b is the extinction coefficient of the compound fully bound to CT-DNA, and K_b is the intrinsic binding constant. The K_b value was given by the ratio of slope to intercept in the plot of [DNA]/(ε_a-ε_f) versus [DNA].

Flow cytometry: Cell death was analysed by measuring the translocation of phosphatidylserine from inner to outer cell membrane. Cells were titrated with compounds for 24 h at 37 °C. Then, they were trypsinised and incubated at 37 °C for 15 min in ABB (140 mM NaCl, 2.5 mM $CaCl_2$, 10 mM Hepes/NaOH, pH 7.4) containing 0.5 mg ml^{-1} of annexin V-DY634. Finally, cells were diluted to 0.5 mL with ABB and analysed by flow cytometry (FACSCalibur, BD Biosciences, Spain).

HeLa (cervical cancer) and Jurkat (leukemia) cell lines were obtained from ATCC, USA.

Acknowledgements

Authors thank the Ministerio de Economía y Competitividad (MINECO-FEDER PID2019-104379RB-C21, PID2019-104379RB-C22/AEI/10.13039/501100011033, RED2018-102471-T (MCIN/AEI/10.13039/501100011033)) and Gobierno de Aragón-Fondo Social Europeo (E07_23R) for financial support. M. Gil-Moles acknowledges support by an FPI-MINECO Fellowship (BES-2014-070407).

Conflict of Interests

The authors declare no conflict of interest.

Data Availability Statement

The data that support the findings of this study are available from the corresponding author upon reasonable request.

Keywords: cancer · cytotoxicity · polynuclear compounds · silver · terpyridine

[1] a) B. Rosenberg, L. VanCamp, J. E. Trosko, V. H. Mansour, *Nature* **1969**, *222*, 385–386; b) R. A. Alderden, M. D. Hall, T. W. Hambley, *J. Chem. Educ.* **2006**, *83*, 728–734.
[2] a) T. C. Johnstone, K. Suntharalingam, S. J. Lippard, *Chem. Rev.* **2016**, *116*, 3436–3486; b) R. Oun, Y. E. Moussa, N. J. Wheate, *Dalton Trans.* **2018**, *47*, 6645–6653.
[3] I. Ott, R. Gust, *Arch. Pharm. Chem. Life Sci.* **2007**, *340*, 117–126.
[4] P. C. A. Bruijnincx, P. J. Sadler, *Curr. Opin. Chem. Biol.* **2008**, *12*, 197–206.
[5] C. S. Allardyce, P. J. Dyson, *Dalton Trans.* **2016**, *45*, 3201–3209.
[6] E. Boros, P. J. Dyson, G. Gasser, *Chem.* **2020**, *6*, 41–60.
[7] A. Bergamo, G. Sava, *Dalton Trans.* **2011**, *40*, 7817–7823.
[8] B. Bertrand, A. Casini, *Dalton Trans.* **2014**, *43*, 4209–4219.
[9] M. Mora, M. C. Gimeno, R. Visbal, *Chem. Soc. Rev.* **2019**, *48*, 447–462.

[10] T. Zou, C. T. Lum, C.-N. Lok, J.-J. Zhang, C.-M. Che, *Chem. Soc. Rev.* **2015**, *44*, 8786–8801.
[11] G. V. Suárez-Moreno, D. Hernández-Romero, O. García-Barradas, O. Vázquez-Vera, S. Rosete-Luna, C. A. Cruz-Cruz, A. López-Monteon, J. Carrillo-Ahumada, D. Morales-Morales, R. Colorado-Peralta, *Coord. Chem. Rev.* **2022**, *472*, 214790.
[12] a) X. Liang, S. Luan, Z. Yin, M. He, C. He, L. Yin, Y. Zou, Z. Yuan, L. Li, X. Song, C. Lv, W. Zhang, *Eur. J. Med. Chem.* **2018**, *157*, 62–80; b) E. Movahedi, A. R. Rezvani, *J. Mol. Struct.* **2018**, *1160*, 117–128; c) W. Sim, R. T. Barnard, M. A. T. Blaskovich, Z. M. Ziora, *Antibiotics.* **2018**, *7*, 93.
[13] a) C. N. Banti, S. K. Hadjikakou, *Metallomics* **2013**, *5*, 569–596; b) A. Altay, S. Caglar, B. Caglar, O. Sahin, *Polyhedron* **2018**, *151*, 160–170; c) U. Kalinowska-Lis, A. Felczak, L. Chęcińska, I. Szabłowska-Gadomska, E. Patyna, M. Małecki, K. Lisowska, J. Ochocki, *Molecules.* **2016**, *21*, 87.
[14] S. K. Raju, A. Karunakaran, S. Kumar, P. Sekar, M. Murugesan, M. Karthikeyan, *German J. Pharm. Biomaterials* **2022**, *1*, 6–28.
[15] a) S. Medici, M. Peana, G. Crisponi, V. M. Nurchi, J. I. Lachowicz, M. Remelli, M. A. Zoroddu, *Coord. Chem. Rev.* **2016**, *325–328*, 349–359; b) M. S. Bashandy, *Int. J. Org. Chem.* **2015**, *05*, 166–190; c) L. Ortego, M. Meireles, C. Kasper, A. Laguna, M. D. Villacampa, M. C. Gimeno, *J. Inorg. Biochem.* **2016**, *156*, 133–144; d) D. Salvador-Gil, L. Ortego, R. P. Herrera, I. Marzo, M. C. Gimeno, *Dalton Trans.* **2017**, *46*, 13745–13755.
[16] a) S. Kankala, N. Thota, F. Björkling, M. K. Taylor, R. Vadde, R. Balusu, *Drug Dev. Res.* **2019**, *80*,188–199; b) N. A. Johnson, M. R. Southerland, W. J. Youngs, *Molecules* **2016**, *22*, 1263; c) M. Zaki, F. Arjmand, S. Tabassum, *Inorg. Chim. Acta* **2016**, *444*, 1–22; d) S. Medici, M. Peana, V. M. Nurchi, M. A. Zoroddu, *J. Med. Chem.* **2019**, *62*, 5923–5943.
[17] a) A. C. G. Hotze, B. M. Kariuki, M. J. Hannon, *Angew. Chem.* **2006**, *45*, 4839–4842; b) G. I. Pascu, A. C. G. Hotze, C. Sanchez-Cano, B. M. Kariuki, M. J. Hannon, *Angew. Chem.* **2007**, *119*, 4452–4456; *Angew. Chem. Int. Ed.* **2007**, *46*, 4374–4378; c) U. McDonnell, J. M. C. A. Kerchoffs, R. P. M. Castineiras, M. R. Hicks, A. C. G. Hotze, M. J. Hannon, A. Rodger, *Dalton Trans.* **2008**, 667–675; d) J. C. Peberdy, J. Malina, S. Khalid, M. J. Hannon, A. Rodger, *J. Inorg. Biochem.* **2007**, *101*, 1937–1945; e) L. Cerasino, M. J. Hannon, E. Sletten, *Inorg. Chem.* **2007**, *46*, 6245–6251; f) Y. Parajó, J. Malina, I. Meistermann, G. J. Clarkson, M. Pascu, A. Rodger, M. J. Hannon, P. Lincoln, *Dalton Trans.* **2009**, 4868–4874; g) A. Oleksi, A. G. Blanco, R. Boer, I. Usón, J. Aymamí, A. Rodger, M. J. Hannon, M. Coll, *Angew. Chem.* **2006**, *118*, 1249–1253; *Angew. Chem. Int. Ed.* **2006**, *45*, 1227–1231; h) S. E. Howson, A. Bolhuis, V. Brabec, G. J. Clarkson, J. Malina, A. Rodger, P. Scott, *Nat. Chem.* **2011**, *4*, 31–36; i) A. D. Richards, A. Rodger, M. J. Hannon, A. Bolhuis, *Int. J. Antimicrob. Agents* **2009**, *33*, 469–472.
[18] a) M. A. Fik, A. Gorczyński, M. Kubicki, Z. Hnatejko, A. Fedoruk-Wyszomirska, E. Wyszko, M. Giel-Pietraszuk, V. Patroniak, *Eur. J. Med. Chem.* **2014**, *86*, 456–468; b) K. Malarz, D. Zych, M. Kuczak, R. Musioł, A. Mrozek-Wilczkiewicz, *Eur. J. Med. Chem.* **2020**, *189*, 456–468; c) A. Winter, M. Gottschaldt, G. R. Newkome, U. S. Schubert, *Curr. Top. Med. Chem.* **2012**, *12*, 158–175.
[19] a) P. J. Steel, C. M. Fitchett, *Coord. Chem. Rev.* **2008**, *252*, 990–1006; b) H. Lin, X. Wu, P. A. Maggard, *Inorg. Chem.* **2009**, *48*, 112039.
[20] a) M. T. Behnamfar, H. Hadadzadeh, J. Simpson, F. Darabi, A. Shahpiri, T. Khayamian, M. Ebrahimi, H. Amiri Rudbari, M. Salimi, *Spectrochim. Acta A Mol. Biomol. Spectrosc.* **2015**, *134*, 502–516; b) C. Metcalfe, C. Rajput, J. A. Thomas, *J. Inorg. Biochem.* **2006**, *100*, 1314–1319; c) S. Rubino, P. Portanova, A. Girasolo, G. Calvaruso, S. Orecchio, G. C. Stocco, *Eur. J. Med. Chem.* **2009**, *44*, 1041–1048.
[21] a) G. Canudo-Barreras, L. Ortego, A. Izaga, I. Marzo, R. P. Herrera, M. C. Gimeno, *Molecules.* **2021**, *26*, 6891; b) I. Mármol, S. Montanel-Perez, J. C. Royo, M. C. Gimeno, M. D. Villacampa, M. J. Rodríguez-Yoldi, E. Cerrada, *Inorg. Chem.* **2020**, *59*, 17732–17745; c) A. Johnson, I. Marzo, M. C. Gimeno, *Dalton Trans.* **2020**, *49*, 11736–11742.
[22] M. Gil-Moles, M. C. Gimeno, J. M. López-de-Luzuriaga, M. Monge, M. E. Olmos, D. Pascual, *Inorg. Chem.* **2017**, *56*, 9281–9290.
[23] M. Bardají, O. Crespo, A. Laguna, A. K. Fischer, *Inorg. Chim. Acta* **2000**, *304*, 7–16.
[24] M. Frik, J. Fernández-Gallardo, O. Gonzalo, V. Mangas-Sanjuan, M. González-Alvarez, A. Del Serrano Valle, C. Hu, I. González-Alvarez, M. Bermejo, I. Marzo, M. Contel, *J. Med. Chem.* **2015**, *58*, 5825–5841.
[25] Q. Zhou, Y.-H. Fu, X. Li, G.-Y. Chen, S.-Y. Wu, X.-P. Song, Y.-P. Liu, C.-R. Han, *Phytochem. Lett.* **2015**, *11*, 296–300.
[26] A. Wolfe, G. H. Shimer, T. Meehan, *Biochemistry* **1987**, *26*, 6392–6396.
[27] a) V. T. Yilmaz, E. Gocmen, C. Icsel, M. Cengiz, S. Y. Susluer, O. Buyukgungor, *J. Biol. Inorg. Chem.* **2014**, *19*, 29–44; b) S. Ramakrishnan, V. Rajendiran, M. Palaniandavar, V. S. Periasamy, B. S. Srinag, H. Krishnamurthy, M. A. Akbarsha, *Inorg. Chem.* **2009**, *48*, 1309–1322.
[28] a) A. Tarushi, G. Psomas, C. P. Raptopoulou, V. Psycharis, D. P. Kessissoglou, *Polyhedron* **2009**, *28*, 3272–3278; b) S. Mukherjee, C. Basu, S. Chowdhury, A. P. Chattopadhyay, A. Ghorai, U. Ghosh, H. Stoeckli-Evans, *Inorg. Chim. Acta* **2010**, *363*, 2752–2761; c) L. Ortego, F. Cardoso, S. Martins, M. F. Fillat, A. Laguna, M. Meireles, M. D. Villacampa, M. C. Gimeno, *J. Inorg. Biochem.* **2014**, *130*, 32–37.
[29] a) H. Diebler, F. Secco, M. Venturini, *Biophys. Chem.* **1987**, *26*, 193–205; b) J. M. Kelly, A. B. Tossi, D. J. McConnell, C. OhUigin, *Nucleic Acids Res.* **1985**, *13*, 6017–6034.
[30] J. Chambers, B. Eaves, D. Parker, R. Claxton, P. S. Ray, S. J. Slattery, *Inorg. Chim. Acta* **2006**, *359*, 2400–2406.
[31] G. M. Sheldrick SHELXL-97, *Program for Crystal Structure Refinement, University of Göttingen, Göttingen, Germany*, **1997**.

Manuscript received: January 13, 2023
Accepted manuscript online: March 16, 2023
Version of record online: May 9, 2023